Quantitative Study of the Effect of the Environment on Macroscopic Quantum Tunneling

D. B. Schwartz, B. Sen, C. N. Archie, and J. E. Lukens
Department of Physics, State University of New York, Stony Brook, New York 11794
(Received 15 July 1985)

Data are presented on the temperature-dependent escape rates of a macroscopic system, a SQUID containing a highly damped Josephson junction, from its metastable state. These data provide the first quantitative confirmation of recent predictions of the exponential effects of temperature and damping on quantum tunneling in macroscopic systems in contrast to previously reported discrepancies. Predicted quantum corrections to thermally activated escape at high temperatures are not observed.

PACS numbers: 03.65.–w, 05.30.–d, 74.50.+r

A Josephson junction in a superconducting loop (SQUID) is a macroscopic system described by a single dynamical variable. Questions have recently been raised concerning the validity of quantum mechanical concepts such as tunneling to such macroscopic variables.[1] Josephson junctions are particularly interesting in this regard since it is possible to fabricate SQUIDs with parameters such that quantum tunneling of the macroscopic variable (MQT) is predicted to dominate thermal effects at experimentally accessible temperatures.[2–13] Recent experiments[14–17] have provided quantitative confirmation of these semiclassical MQT predictions in the limit where interactions of the macroscopic variable with the environment, consisting of the many microscopic degrees of freedom in the system, could be neglected. In this Letter we report observations of MQT in a highly damped SQUID where the environment in the form of finite temperature and strong damping is predicted to be a dominant factor in the determination of the tunneling rates.

Classically, the behavior of a SQUID containing an ideal resistively shunted Josephson junction with shunt resistance R, capacitance C, and critical current I_c in a loop of inductance L is given by

$$C\ddot{\Phi}+\dot{\Phi}/R-\partial U/\partial\Phi, \tag{1}$$

where the potential is given by

$$U=\frac{(\Phi-\Phi_x)^2}{2L}-\frac{I_c\Phi_0}{2\pi}\cos\left(\frac{2\pi\Phi}{\Phi_0}\right).$$

The flux linking the loop is Φ; the applied flux, Φ_x; and the flux quantum, Φ_0. This equation is the same as that for a particle of mass C and position Φ moving through a viscous medium with damping $1/R$ in a potential U. In general, U contains a number of metastable minima. As the applied flux is increased the barrier height decreases until at some critical flux, Φ_{xc}, the local minimum becomes an inflection point where, in the absence of any fluctuations, the "particle," which is trapped in the metastable minimum, would roll until trapped by another minimum of the potential—the spacing between minima being approximately Φ_0. For $\Delta\Phi_x\equiv\Phi_{xc}-\Phi_x \ll \Phi_{xc}$ (the region of interest in this experiment) the barrier height is given by

$$\Delta U=[4/3(\pi\beta)^{1/2}](\Phi_0^2/L)\Delta\phi_x^{3/2},$$

where $\beta=2\pi LI_c/\Phi_0$ and $\Delta\phi_x$ is $\Delta\Phi_x$ expressed in units of the flux quantum.

A schematic diagram of the experiment, which uses a technique previously developed for the study of thermal activation in these systems,[18] is shown in Fig. 1. A current applied to one of the coils increases the applied flux Φ_x at a constant rate, decreasing the energy barrier until a decay is observed. A magnetometer coupled through a second coil detects the total flux Φ through the SQUID, the signature of a decay being the abrupt transition in Φ by about Φ_0. In an experimental run approximately 10^4 transitions are measured. The results of these measurements are then formed into a

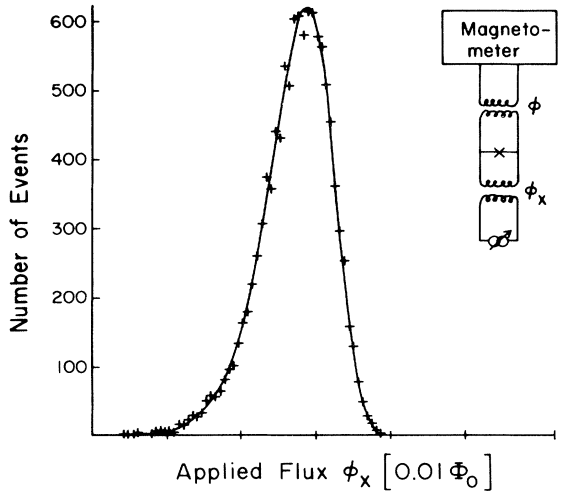

FIG. 1. Typical histogram representing the tunneling probability distribution. The inset is a schematic diagram of the experiment.

histogram, as shown in Fig. 1, which when suitably normalized is just the probability distribution of the transitions. This distribution is a product of an exponentially increasing escape rate $\Gamma(\Phi_x)$ as $\Delta\Phi_x \rightarrow 0$ and the rapidly decreasing number of populated systems for large Γ.[19]

The SQUID studied in this work is fabricated from a small-area Pb-alloy edge junction (area $\sim 0.1\ \mu m^2$) shunted by a Pd thin-film resistor ($R = 9 \pm 1\ \Omega$) placed within 2 μm of the junction. The calculated series inductance of less than 3 pH gives an inductive cutoff for the shunt resistor greater than 500 GHz. Bounds on the junction capacitance C are estimated, both from the area[20] and from the deviation from thermal activation at 2 K of an unshunted junction with the same area and critical current, to be $6\ \text{fF} < C < 14$ fF. The SQUID is formed by a 10-μm-wide Pb strip laid around the perimeter of a 250-μm square bisected by a 40-μm-wide Pb strip connected to the junction at the center of the square. The effective SQUID inductance has been independently measured to be 270 ± 30 pH. The SQUID and the flux transformers which couple it to the magnetometer and field coils (Fig. 1) are fabricated on a sapphire substrate in a single deposition. A ^{4}He-filled NbTi cell with narrow channels connecting it to a sintered copper heat exchanger provides good thermal contact while maintaining the integrity of the superconducting magnetic shielding. This cell is placed on a platform shared with a heater and resistance secondary thermometer for temperature regulation. A ^{3}He melting-curve cell on the same platform serves as the primary thermometer, providing an absolute temperature accuracy of $\pm 1\% \pm 1$ mK over the experimental temperature range of $10\ \text{mK} \leq T \leq 730$ mK. The platform is cooled by a dilution refrigerator. Extensive efforts have been made to shield the sample from all external noise.

At high temperatures the decay of the metastable states is by thermal activation over the barrier with the rate given by

$$\Gamma(T, \Phi_x) = \omega_T \Pi_q \exp(-\Delta U/k_B T), \quad (2)$$

where $\Pi_q = 1$ for temperatures sufficiently high that tunneling through the barrier is negligible so that the classic Kramers result holds. For the junction discussed here, the undamped small oscillation frequency is $\omega_0 \sim 1.2 \times 10^{12}\ \text{s}^{-1}$ and the RC cutoff frequency $\gamma \equiv 1/RC \sim 1.1 \times 10^{13}\ \text{s}^{-1}$. In the high-damping limit, $\gamma >> \omega_0$, appropriate to these measurements $\omega_T = \omega_0^2/(2\pi\gamma)$. Thus the thermal attempt frequency is $\omega_T \sim 21$ GHz and is given in terms of the junction parameters by $\omega_T = (\beta/\pi)^{1/2}(R/L)\Delta\phi_x^{1/2}$. Note that this result is independent of C and, thus, for highly damped systems does not involve ω_0. Recent work suggests that significant quantum corrections to thermal activation (QCTA) extend to temperatures many times the crossover temperature to thermal-activation–dominated escape. The effect of these corrections is to increase the escape rate, i.e., $\Pi_q > 1$ in Eq. (2).[3,6,8,10,13]

At zero temperature, where the thermal escape rate goes to zero, it is predicted that the escape from the metastable well will be via quantum tunneling[2,4] with

$$\Gamma(0) = \omega_Q \exp(-B_Q), \quad (3)$$

where for high damping $B_Q = \frac{3}{2}(\Delta U/\hbar\omega_T)$ and is given in terms of sample parameters by $B_Q = (\pi/\beta)(R_0/R)\Delta\phi_x \equiv B_{Q0}\Delta\phi_x$ with $R_0 \equiv h/e^2 = 2.59 \times 10^4\ \Omega$. The prefactor ω_Q has been calculated numerically with the result $\omega_Q = 5 \times 10^{15}\ \text{s}^{-1}$ for the parameters of the sample studied here.[7] Quantum tunneling is predicted to be the dominant escape mechanism below a crossover temperature $T_0 = \hbar\omega_T/k_B$.[5] For temperatures below T_0, the predicted effect of the heat bath is to increase the escape rate so that Γ contains a temperature dependence[5,9] giving

$$\Gamma(T) = \Gamma(0)\exp[(T/T_Q)^2], \quad 0 < T < T_0. \quad (4)$$

The scale factor T_Q is given in terms of the sample parameters by

$$T_Q = \frac{\sqrt{12}}{\pi^2}\frac{\beta\Phi_0^2}{Lk_B}\left(\frac{R}{R_0}\right)^{3/2}.$$

The quantum calculations are valid in the semiclassical limit requiring that the particle be well localized near the potential minimum. This criterion, which can be expressed as $\Delta U >> h\omega_T$,[4,21] is well satisfied for the data presented here.

The high-temperature thermal-activation rate ($\Pi_q = 1$), the quantum exponent B_Q, and the finite-temperature tunneling enhancement are all independent of the junction capacitance in the high-damping limit and only sensitive to frequencies below about the thermal attempt frequency ω_T,[7] since the action cuts off as $\exp(-\omega/\pi\omega_T)$—at a frequency of about 10 GHz for this sample. Since the sample inductance and resistance are well characterized by their lumped values and the intrinsic junction dissipation is negligible to frequencies well above ω_T, our measurements should provide a critical test of these aspects of the theory. In contrast, the quantum prefactor for $T = 0$, ω_Q, as well as Π_q, the quantum correction above T_0, are both much more sensitive to the detailed high-frequency response of the system, depending as a low power law on the capacitance and responding to frequencies of at least order γ.[8]

To within the precision of these measurements the shape of the distribution (Fig. 1) does not depend on the form of the escape rate in Eqs. (2)–(4). Thus, all available information from the escape rates is contained in the mean $\bar{\Phi}_x$ and the width σ_x of the distri-

butions. These quantities are shown versus temperatures in Figs. 2 and 3. The qualitative signatures of quantum tunneling, the approach of $\bar{\Phi}_x$ and σ_x to finite values as $T \rightarrow 0$, are clearly evident from these plots. Detailed discussions of relationship of the parameters in the escape-rate equations to the mean and width of the distribution have been given elsewhere.[22] The essential dependencies can, however, be seen rather simply: Below T_0, where B_Q depends linearly on Φ_x, $\sigma_x^{-1} \propto \partial \ln\Gamma/\partial\Phi_x$. Thus, the width gives a direct measure of B_{Q0}. Since data are always taken for essentially the same range of Γ, any change in the parameters which tends to change Γ will be compensated for by a change in the mean. Thus, changes in quantities such as ω_Q, temperature, and Φ_{xc} which change Γ but are not coefficients of Φ_x will only cause changes in the mean. Note that, in particular, a T^2 variation in $\ln\Gamma$ from Eq. (4) would cause a T^2 variation in the mean but no change in σ_x.

Figures 2 and 3 show the comparison of these data with various theories throughout the temperature range. The junction parameters have been independently determined. However, the precision of the data is in general better than the accuracy of these determinations; thus in the analysis below we treat these parameters as fitting parameters to be compared with their independent determinations. As can be seen, the variation of the $\bar{\Phi}_x$ and σ_x with temperature for $T < T_0$ is well described by Eqs. (3) and (4). In particular the temperature independence of σ_x follows from the temperature independence of B_{Q0}. In addition, since the mean is temperature dependent in this region, the constancy of σ_x implies a linear dependence of B_Q on Φ_x. The value for the junction resistance of $R = 8\ \Omega$ determined by $\sigma_x(0)$ is in good agreement with the independent estimate of $9 \pm 1\ \Omega$ based on the measurement of a current-biased test junction fabricated simultaneously with the SQUID. This zero-temperature width is a factor of 4 less than that obtained with an unshunted SQUID with nearly the same area and critical flux and with a crossover temperature of about 2 K. The predicted T^2 variation of $\bar{\Phi}_x$ from Eq. (4) is clearly seen in the excellent fit (with use of $L = 253 \pm 3$ pH as the fitting parameter) of $\bar{\Phi}_x$ to a parabola shown in Fig. 2(b) over the entire range $0 < T < T_0$. As can be seen, the values found for these fitting parameters agree with their independently determined values to within the experimental accuracy. These results represent *quantitative* confirmation of the predicted suppression of low-temperature quantum tunneling by dissipation and also provide the initial test of theories of macroscopic quantum tunneling in the high damping limit. Both the functional forms and magnitudes of the exponents in Eqs. (3) and (4) agree with theory.

The exact value of Φ_{xc}, where the energy barrier vanishes, serves only to change the value of ω_Q but does not affect the fit to either the width or the mean below T_0. Assuming the predicted value of the quantum prefactor $\omega_Q = 5 \times 10^{15}\ \mathrm{s}^{-1}$ gives a fit of the suppression of the mean flux below Φ_{xc} at $T = 0$ to be $\Delta\bar{\Phi}_x(0) = (0.077 \pm 0.002)\Phi_0$.[23] An independent determination of Φ_{xc} has been made through a measurement of the nonlinear component of the Φ vs Φ_x response curve for $\Phi_x < \bar{\Phi}_x$. Since $\partial\Phi/\partial\Phi_x \rightarrow \infty$ as $\Phi_x \rightarrow \Phi_{xc}$ this measurement, which will be described in detail elsewhere, provides a very sensitive measure of the difference $\Delta\bar{\Phi}_x$ between $\bar{\Phi}_x$ and Φ_{xc}, giving $\Delta\bar{\Phi}_x(0) = (0.050 \pm 0.010)\Phi_0$. The fitted and measured values of Φ_{xc} *do not agree*. This measured value of $\Delta\bar{\Phi}_x(0)$ implies $\omega_Q = 3 \times 10^{10}\ \mathrm{s}^{-1} \sim \omega_T$. Further, it can be seen from Fig. 2(a) that in the region above T_0 the predictions of QCTA even with use of the best-fit parameters do not agree with the data. Note that Φ_{xc}

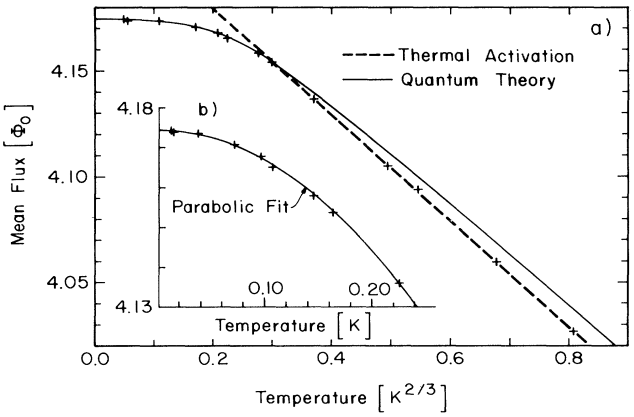

FIG. 2. (a) Mean ($\bar{\phi}_x$) of the escape distribution vs $T^{2/3}$ shown with best fit to (dashed curve) thermal activation and (solid curve) quantum theory. (b) Parabolic fit of $\bar{\phi}_x$ vs T for $T < T_0$.

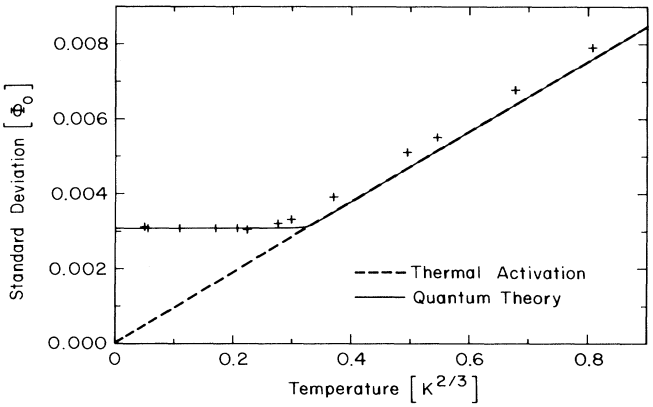

FIG. 3. The variation of the width (σ_x) of the escape probability distribution vs $T^{2/3}$ compared with (dashed curve) thermal activation and (solid curve) quantum theory.

acts mainly to shift the entire curve along the $\bar{\Phi}_x$ axis but does not significantly alter its shape. The quantities for which theory does not fit the data, ω_Q and Π_q, are just those prefactors whose calculation depends on the high-frequency response of the junction dissipation.

As can be seen from Fig. 2(a) the fit to the uncorrected thermal activation result [$\Pi_q = 1$ in Eq. (2)] using L and Φ_{xc} as adjustable parameters describes the data above T_0 extremely well. Further, the fitting parameter $\Phi_{xc} = \overline{\Delta\Phi_x}(0) + (0.049 \pm 0.001)\Phi_0$ now *agrees* with the measured value. In addition the best-fit value of $L = 253 \pm 3$ pH from thermal activation is consistent with a value of $L = 258 \pm 12$ pH obtained from T_Q in fitting Eq. (4) below T_0.

As can be seen in Fig. 3 the predicted width $\sigma_x(T)$ above T_0 is essentially the same whether or not quantum corrections are included. The measured widths above T_0 are all about $3 \times 10^{-4}\Phi_0$ greater than predicted. This offset, which is about twice the instrumental resolution, is presently not understood. The cause of the discrepancies noted above between the predicted and measured values of the prefactors also remains unexplained. The effects of a number of possible deviations in the sample impedance for $\omega \sim \gamma$ (e.g., the parasitic shunt inductance) have been calculated. While these cannot explain the observed discrepancy (and in fact can make it worse) we do not presently rule out the possibility that some such effect may be significant in understanding these deviations.

We conclude that in a well-characterized macroscopic quantum system, where parameters are independently determined, excellent agreement is obtained with both the functional forms and the magnitudes of the quantum exponents. In particular, in the high-damping limit, the magnitude, temperature dependence, and dependence on barrier height (through $\Delta\Phi_x$) for both the zero-temperature exponent and the finite-temperature correction below T_0 agree with theoretical predictions evaluated with use of the independently determined parameters. The data are, however, not in agreement with those aspects of the theory which are sensitive to the details of the junction response at frequencies of order γ, namely ω_Q, and the closely related quantum corrections to thermal activation above T_0. In fact, above T_0, the data are much better described by classical thermal activation.

We wish to acknowledge useful discussions with S. Chakravarty, L.-D. Chang, H. Grabert, P. Hanggi, S. Kivelson, A. J. Leggett, and A. Schmid, and to thank K. Springer for help with the sample fabrication, as well as to acknowledge the assistance provided by Dr. A. Jain in many aspects of this work. The work was supported by the National Science Foundation through Grants No. DMR 8303982 and No. DMR 8218993. Initial support as well as support for the facilities used in the work was provided by the U.S. Office of Naval Research.

[1]A. J. Leggett, Contemp. Phys. **25**, 583 (1984).

[2]A. O. Caldeira and A. J. Leggett, Phys. Rev. Lett. **46**, 211 (1981).

[3]P. G. Wolnyes, Phys. Rev. Lett. **47**, 968 (1981).

[4]A. O. Caldeira and A. J. Leggett, Ann. Phys. **149**, 374 (1983).

[5]A. I. Larkin and Yu. N. Ovchinnikov, Pis'ma Zh. Eksp. Teor. Fiz. **37**, 322 (1983) [JETP Lett. **37**, 383 (1983)].

[6]V. I. Mel'nikov and S. V. Meshkov, Pis'ma Zh. Eksp. Teor. Fiz. **38**, 111 (1983) [JETP Lett. **38**, 130 (1983)].

[7]L.-D. Chang and S. Chakravarty, Phys. Rev. B **29**, 130 (1984); **30**, 1566(E) (1984).

[8]A. I. Larkin and Yu. N. Ochinnikov, Zh. Eksp. Teor. Fiz. **86**, 719 (1984) [Sov. Phys. JETP **59**, 420 (1984)].

[9]H. Grabert, U. Weiss, and P. Hanggi, Phys. Rev. Lett. **52**, 2193 (1984).

[10]H. Grabert and U. Weiss, Phys. Rev. Lett. **53**, 1787 (1984).

[11]A. J. Leggett, Phys. Rev. B **30**, 1208 (1984).

[12]H. Grabert, P. Olshowski, and U. Weiss, to be published.

[13]P. Hanggi, J. Stat. Phys. (to be published).

[14]R. F. Voss and R. A. Webb, Phys. Rev. Lett. **47**, 265 (1981).

[15]L. D. Jackel, J. P. Gordon, E. L. Hu, R. E. Howard, L. A. Fetter, D. M. Tennant, R. W. Epworth, and J. Kurkijärvi, Phys. Rev. Lett. **47**, 697 (1981).

[16]J. Martinis, D. Esteve, M. Devoret, and J. Clarke, private communication.

[17]S. Washburn, R. A. Webb, R. F. Voss, and S. M. Faris, Phys. Rev. Lett. **54**, 2712 (1985).

[18]L. D. Jackel, W. W. Webb, J. E. Lukens, and S. S. Pei, Phys. Rev. B **9**, 115 (1972).

[19]J. Kurkijärvi, Phys. Rev. B **6**, 832 (1972).

[20]J. H. Magerlein, IEEE Trans. Magn. **17**, 286 (1981).

[21]S. Kivelson, private communication.

[22]J. Kurkijärvi, in *SQUID: Superconducting Quantum Interference Devices and their Applications,* edited by H. D. Hahlbohm and H. Lubbig (de Gruyter, Berlin, 1980), p. 247; also see D. B. Schwartz, B. Sen, C. N. Archie, A. K. Jain, and J. E. Lukens, in *Proceedings of the First International Conference on SQUID's, Berlin, 1985,* edited by H. D. Halbohm and H. Lubbig (de Gruyter, Berlin, 1985), p. 53, where a preliminary discussion of this work may be found.

[23]The effect of the weak dependence of the rate on the capacitance, within stated limits, is to change slightly the best-fit value of Φ_{xc}; thus the uncertainty in C is accounted for in the error limits on the fitting parameter Φ_{xc}.